

MODELLING AND UNCERTAINTY FOR HIGH-ACCURACY ROUNDNESS MEASUREMENT

*Maurice G. Cox*¹ and *Annarita Lazzari*²

¹Mathematics and Scientific Computing Group, National Physical Laboratory, Teddington, UK

²Mitutoyo Institute of Metrology, Mitutoyo Italiana, Milan, Italy

Abstract – High-accuracy roundness measurements of a component made with an instrument having a precision rotary stage are considered. The measurements comprise a superimposition of the component form deviation and the instrument spindle deviation, the latter being a consequence of the imperfect but highly repeatable rotation of the sensor. These effects need to be separated in order to determine the departure from roundness of the component, and also of the spindle deviation. Separation is possible by using the rotary stage to take several sets of measurements, corresponding to different angular positions of the component with respect to the rotary stage, which introduces phase differences relative to these effects. The evaluation of the uncertainty associated with the departures from roundness is the main concern. When the measurements are uncorrelated, the evaluation provides specific formulae for the uncertainty. For the instrument of concern, the presence of serial correlations in the measurements means that the uncertainties so evaluated would be too small. An approach based on the use of bootstrap re-sampling is given that permits the correlation effects to be taken into account. Results are provided for comparison with those obtained based on the assumption that the measurements are uncorrelated.

Keywords roundness form deviation separation, correlated measurements, uncertainty evaluation

1. INTRODUCTION

A roundness-measuring instrument with a precision rotary stage [1], [2] is used to establish the profile, and hence the departure from roundness of the profile, of a nominally circular section of a workpiece.¹ The instrument sensor does not rotate perfectly, although in a highly repeatable way, having a systematic angle-dependent spindle deviation. An indexing stage is used to rotate the workpiece through any specified angle before measurement. Measurement traces, each consisting of, say, 2000 suppressed-radius values, taken for each of several positions of the stage, are used to determine the angle-dependent component form deviation (CFD) and the instrument spindle deviation (ISD) in terms of their Fourier harmonics.

The measurement uncertainties associated with these deviations are evaluated. The considerations relate to a Type A evaluation of uncertainty, i.e., based on an analysis of a series of measurements.²

The measured traces comprise a superimposition of CFD and ISD. A trace $Y(\theta)$, say, is thus of $C(\theta) + S(\theta)$, $C(\theta)$ denoting the CFD, $S(\theta)$ the ISD, and θ the angular position of the indexing stage.

By rotating the workpiece through indexing angles ϕ_1, \dots, ϕ_q , q traces having the form

$$\begin{aligned} Y^{(1)}(\theta) &= C(\theta - \phi_1) + S(\theta), \\ &\dots \\ Y^{(q)}(\theta) &= C(\theta - \phi_q) + S(\theta) \end{aligned} \quad (1)$$

are obtained.³ It is required to extract $C(\theta)$ and $S(\theta)$, given the measurement traces $Y^{(\ell)}(\theta)$, $\ell = 1, \dots, q$.

An approach for determining $C(\theta)$ and $S(\theta)$ and associated uncertainties is described. It applies to arbitrary indexing angles and uncorrelated measurements, and generalizes previous work for uniformly [1] and non-uniformly spaced angles [2]. It is based on the use of a measurement model and the law of propagation of uncertainty [3], and summarized as follows:

1. Form the Fourier harmonics for each trace $Y^{(\ell)}(\theta)$ and the associated uncertainties.
2. Express $C(\theta)$ and $S(\theta)$ algebraically as Fourier series with adjustable coefficients.
3. Use expression (1) to construct a model relating these Fourier representations and solve it for the Fourier harmonics of $C(\theta)$ and $S(\theta)$. Evaluate the uncertainties associated with these harmonics.
4. Evaluate the uncertainties associated with values of $C(\theta)$ and with the departure from roundness $\max_{\theta} C(\theta) - \min_{\theta} C(\theta)$, and similarly for $S(\theta)$.

² A Type B evaluation, accounting for other effects, has been carried out separately by the instrument designers.

³ A previous stage in the measurement procedure ensures that the workpiece is accurately centred.

¹ Strictly, an *estimate* of the real profile is established.

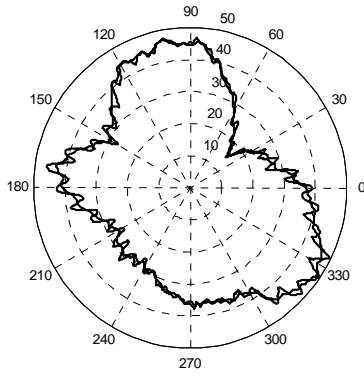


Figure 1. A typical trace (broken curve) and the constructed 'model trace'. The radial axis is in nm.

This approach is not applicable if the

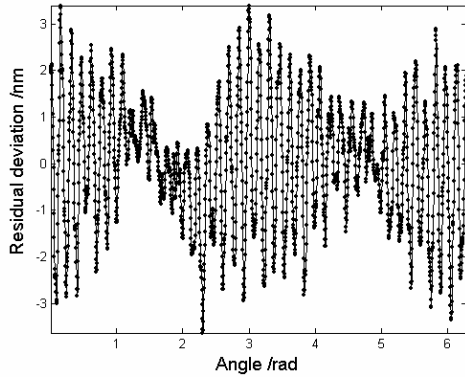


Figure 2. Residual deviations, joined by straight-line segments to show their behaviour more clearly, derived from the measurement and 'model' traces in figure 1.

measurements have appreciable correlation. Ignoring such correlations, which are positive in practice, would lead to a gross underestimate of the uncertainties in step 4. That the measurement deviations are uncorrelated is an extremely poor assumption for the instrument of concern here, the ultra-high precision NPL-Taylor Hobson Talyron 73HPR roundness-measuring instrument.

Figure 1 shows a typical measurement trace, as a polar plot, and the corresponding 'model trace', the trace constructed from the Fourier coefficients determined by the above process. In general terms the model trace reproduces the measured trace, but the residual deviations, viz., the radial departures of the measured trace from the model trace, exhibit highly systematic behaviour. Figure 2, a Cartesian plot showing these deviations as a function of angular position, highlights this behaviour. The behaviour is very different from that of Gaussian noise, say: the deviations are strongly serially correlated. Similar behaviour is observed for all measurement traces provided by this instrument.

Although the measured traces can each individually be well represented by a Fourier series, the same is not true for the traces constructed from the Fourier series determined for $C(\theta)$ and $S(\theta)$. The reason is two-fold. First, these two Fourier series have a number of Fourier coefficients that is much smaller than the total number of measurements in the original traces. Second, and more importantly, the nature of the measurement deviations in the traces is such that they can be closely modelled individually but not collectively by Fourier series.

A treatment based on the above four steps is given for cases where the measurements are regarded as random and uncorrelated (section 0). A treatment that accounts for the serial correlation effects observed for the 73HPR measurements is then considered (section 3). The application of both approaches to measurements of the profile of a section of a glass hemisphere is given (section 4).

2. UNCORRELATED MEASUREMENTS

Consider roundness-measuring instruments for which the measurement deviations can be regarded as uncorrelated and identically distributed, with (unspecified) associated standard uncertainty $u(y)$. Algebraic results and the associated uncertainties are given for $C(\theta)$ and $S(\theta)$ in this case. Derivations are provided in the appendix. The following steps relate to those in section 1.

1. Denote the suppressed-radius measurements in the ℓ th trace $Y^{(\ell)}(\theta)$, say, by $y_i^{(\ell)}$, at angles $\theta_i = 2\pi(i-1)/m$, $i = 1, \dots, m$. For $\ell = 1, \dots, q$, use the Fast Fourier Transform [4] to represent $y_i^{(\ell)}$, $i = 1, \dots, m$, by the n -harmonic Fourier series⁴

$$Y_n^{(\ell)}(\theta) \approx a_0^{(\ell)} + \sum_{k=1}^n (a_k^{(\ell)} \cos k\theta + b_k^{(\ell)} \sin k\theta). \quad (2)$$

The standard uncertainty associated with each coefficient $a_k^{(\ell)}$ and $b_k^{(\ell)}$, $k = 1, \dots, n$, is [5]

$$u(a_k^{(\ell)}) = u(b_k^{(\ell)}) = (2/m)^{1/2} u(y),$$

and $u(a_0^{(\ell)}) = (1/m)^{1/2} u(y)$.⁵ All covariances associated with these coefficients are zero.

2. Represent $C(\theta)$ and $S(\theta)$, respectively, by the n -harmonic Fourier series

$$C_n(\theta) = \alpha_0 + \sum_{k=1}^n (\alpha_k \cos k\theta + \beta_k \sin k\theta), \quad (3)$$

⁴ See section 4 regarding the choice of n .

⁵ The standard uncertainty associated with the constant terms in the Fourier representations is, however, equal to $(1/m)^{1/2} u(y)$, but these terms are of no consequence here.

$$S_n(\theta) = \gamma_0 + \sum_{k=1}^n (\gamma_k \cos k\theta + \delta_k \sin k\theta). \quad (4)$$

3. Determine the Fourier coefficients α_k , β_k , γ_k and δ_k as described in the appendix. The associated standard uncertainties are given by

$$\begin{aligned} u^2(\alpha_k) &= u^2(\beta_k) = u^2(\gamma_k) = u^2(\delta_k) \\ &= \frac{2q}{m(q^2 - \mu_k^2)} u^2(y), \end{aligned} \quad (5)$$

where

$$\begin{aligned} \mu_k^2 &= c_k^2 + s_k^2, \\ c_k &= \sum_{\ell=1}^q \cos k\phi_\ell, \quad s_k = \sum_{\ell=1}^q \sin k\phi_\ell. \end{aligned}$$

4. Form the standard uncertainty associated with a value of $C_n(\theta)$:

$$u(C_n(\theta)) = (2/m)^{1/2} \tau u(y), \quad (6)$$

where

$$\tau^2 = q \sum_{k=1}^n \frac{1}{q^2 - \mu_k^2}, \quad (7)$$

a result that is independent of θ .⁶ Let $C_n = C_n(\theta)$. Form the component departure from roundness

$$\delta C = C_n(\theta_{\max}) - C_n(\theta_{\min}), \quad (8)$$

where θ_{\max} and θ_{\min} are the angles at which $C_n(\theta)$ takes its maximum and minimum values, respectively, with an analogous result for the spindle departure from roundness. Form the associated standard uncertainty

$$u(\delta C) \leq 2u(C_n) = 2(2/m)^{1/2} \tau u(y). \quad (9)$$

3. CORRELATED MEASUREMENTS

The uncertainty evaluation in section 0 would be valid for instruments that provided traces consisting of uncorrelated measurements. That approach could be adapted to correlated measurements if the covariance effects could be quantified, but such information is not directly available from knowledge of the instrument.

An approach is used, and applied in section 4, that makes no assumption concerning the distribution of the residual deviations. In particular, it does not require covariances to be quantified. This approach is bootstrap re-sampling, used successfully in other problems in metrology [6], [7].

One implementation of bootstrap re-sampling would first generate ‘new’ traces as the sum of the model traces and re-sampled residual deviations.⁷ Then, the solution, and especially the corresponding values of δC and δS , would be determined for these ‘new’ traces. By re-sampling many times, approximate distributions for the values of δC and δS would be produced, from which the required uncertainties would be evaluated.

This implementation of bootstrap re-sampling is inapplicable, however, because it would destroy the structure of the residual deviations and hence the serial correlation present. Instead, re-sampling can be carried out at the trace level rather than at the level of the individual points in each trace. In this way the uncertainty structure in the different traces is retained, but, by randomly selecting traces, with replacement from the complete set of measurement traces, ‘new’ complete roundness data sets having characteristics consistent with those of the measured traces can be generated.

A moderately large number M (= 10 000, say) of trials is made. Each trial consists of a complete re-sampled roundness data set. The M trials constitute a simulation. For each of the above sets the complete problem is solved as in section 0 (without evaluating the uncertainties), assigning the correct index angle to each re-sampled trace.

For the example in section 4, there are $q = 22$ traces, indexed by 1, 2, ..., 22. An instance of the traces used for one of the trials (the last in fact) was 17, 9, 22, 3, 13, 3, 19, 9, 17, 6, 14, 17, 16, 7, 12, 15, 1, 13, 16, 7, 16, 8. When sorted, these indices are 1, 3, 3, 6, 7, 7, 8, 9, 9, 12, 13, 13, 14, 15, 16, 16, 16, 17, 17, 17, 19, 22, indicating that original trace 1 was used, as was trace 3 (twice), trace 6, etc. Original traces 16 and 17 were in fact each used three times. Eight of the original traces (2, 4, 5, 10, 11, 18, 20, 21) were not used at all.

The result of the simulation is M realizations of the value of δC and similarly of δS , the out-of-roundness quantities. These realizations are used to provide approximations to the distribution functions for the values of δC and δS [7]. The expectation (mean) of the distribution function for the value of δC is taken as the estimate of the value of δC , the standard deviation as the standard uncertainty $u(\delta C)$ associated with the estimate, and the shortest coverage interval for the value of δC corresponding to a coverage probability of 95 % (say) extracted [7]. An analogous statement applies to δS .

⁶ The same result holds for $S_n(\theta)$ for the ISD.

⁷ A re-sampled residual deviation is a residual deviation chosen as random from the residual deviations for a trace.

Histograms of each set of realizations can also be used, when appropriately scaled, to provide approximate probability density functions (PDFs) for the values of the CFD and ISD [7]. Such PDFs are useful in visualizing key aspects of the manner in which the values of the quantities concerned are distributed, e.g., the tail behaviour and any asymmetry.⁸ However, the approximations to the distribution functions are better suited to providing the above numerical values.

4. RESULTS

The approach of section 0 was applied to measurements of $q = 22$ traces, each containing $m = 2\,000$ radial measurements, of the profile of a section of a glass hemisphere. Non-uniformly spaced indexing angles were chosen.⁹ $n = 150$ Fourier harmonics were obtained.¹⁰ The root-mean-square residual deviations for the Fourier representations of the traces lay between 0.30 nm and 0.35 nm, with a mean value of 0.33 nm, which

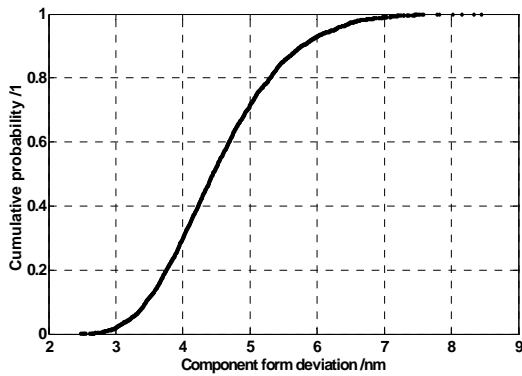


Figure 3. Approximation to the distribution function for the value of the component form deviation.

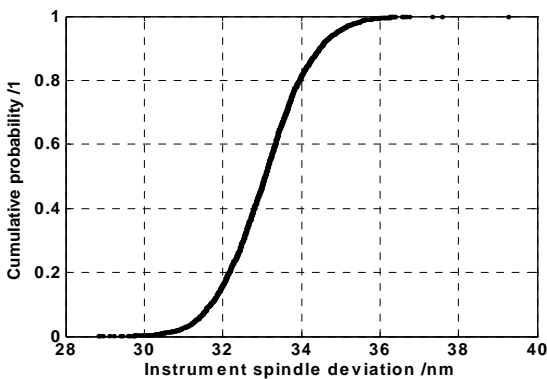


Figure 4. Approximation to the distribution function for the value of the instrument spindle deviation.

estimates the standard uncertainty $u(y)$.

For the choice made of indexing angles, τ , defined by expression (7), was equal to 2.8. Using expression (9), the standard uncertainty associated with the estimate of the departure from roundness is

$$u(\delta C) \leq 2 \times (2/2\,000)^{1/2} \times 2.8 \times 0.33 \approx 0.06 \text{ nm.}$$

This value is exceedingly small,¹¹ even for ultra-high accuracy roundness measurement, and hence the basic assumption behind the uncertainty evaluation is highly questionable.

The simulation approach of section 3 was then applied. $M = 10\,000$ bootstrap trials were made, on the basis of which the approximations to the distribution functions for the values of δC and δS shown in figures 3 and 4 were obtained.

Approximate probability density functions (PDFs) [7] for the values of the CFD and ISD were also formed (figures 5 and 6). They were each determined by first constructing a histogram (with

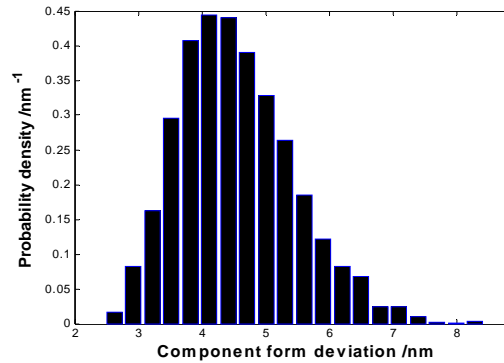


Figure 5. Approximate PDF for the value of the component form deviation.

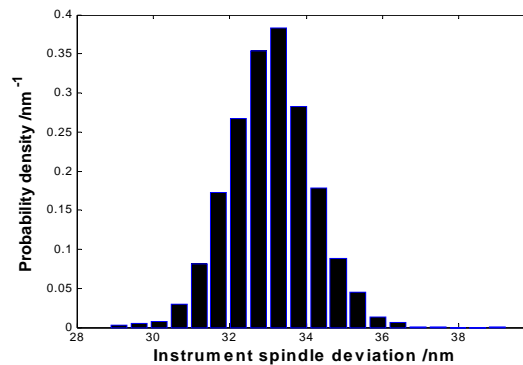


Figure 6. Approximate PDF for the value of the instrument spindle deviation.

⁸ Both these aspects influence the coverage intervals for the values of the CFD and the ISD.

⁹ The use of appropriately chosen index angles avoids harmonic-suppression problems [2].

¹⁰ This choice of n is related to the filtering characteristics of the instrument, and is appropriate for sphere measurement.

¹¹ It would be even smaller were the above correlation coefficient appreciably less than unity.

20 bins) of the 10 000 values, and then converting them to a bar chart by applying a scaling factor such that the resulting chart had unit area.

The approximate PDF for the value of the CFD is asymmetric, whereas that for the ISD seems to be symmetric. Since the value of the CFD is much closer to zero than that of the ISD (relative to the associated standard uncertainties), such behaviour might be anticipated. A symmetric PDF that can take all possible real values, such as a Gaussian distribution, would, with some non-zero probability, take negative values. A PDF for the value of a positive quantity, such as the departure from roundness here, that is close to the origin is necessarily asymmetric. Differences in the corresponding distribution functions (figures 3 and 4) can also be seen, in terms of the tail behaviour, for instance. However, the shapes of (approximate) PDFs are more sensitive to underlying differences.

The estimates, associated standard uncertainties and coverage intervals obtained from the approximations to the distribution functions are given in table 1, in which $[a, b]$ denotes the shortest coverage interval¹² with endpoints a and b corresponding to a 95 % coverage probability [7].

Table 1. Departure from roundness values from simulation.

	Estimate	Standard uncertainty	Coverage interval
δC /nm	4.5	0.9	[3.0, 6.4]
δS /nm	33.1	1.1	[30.9, 35.2]

These results can be compared with those above under the (invalid) assumption that the measurements are uncorrelated. There, $u(\delta C) = u(\delta S) = 0.06$ nm was obtained, compared with the above standard uncertainties of 0.9 nm and 1.1 nm. The latter values are close to the Type A standard uncertainties anticipated by the designers of the instrument; the basic sensor resolution is 1.2 nm. Also, they are comparable to the Type B standard uncertainties associated with the measurements, as also expected.

5. CONCLUSIONS

The departure from roundness of the profile of a section of a workpiece can be determined from measurement traces determined with an instrument having a precision rotary stage. Measurement traces corresponding to different angular positions of the component with respect to the rotary stage provide a basis for separating the component form deviation from the instrument spindle deviation. The

associated uncertainties can be evaluated using a straightforward, but algebraically complicated, application of the law of propagation of uncertainty in cases where the measurements are uncorrelated. For the instrument of concern, the measurements are strongly serially correlated. By not taking account of this effect, the resulting uncertainties are grossly underestimated. The law of propagation of uncertainty cannot readily be applied in this instance, because the covariances associated with the measurements are not directly available. An alternative approach is described that treats this effect using bootstrap re-sampling in a way that preserves the serial correlation. The resulting uncertainty proves to be much more realistic.

David Flack and Peter Harris (NPL) and Mike Mills (Taylor Hobson) made valuable input at various stages of this work.

REFERENCES

- [1] C. P. Reeve. The calibration of a roundness standard. Report NBSIR 79, National Bureau of Standards, 1979.
- [2] C. Linxiang, W. Hong, L. Xiongua and S. Qinghing. Full-harmonic error separation technique. *Meas. Sci. Technol.*, **3**, 1129–1132, 1995.
- [3] BIPM *et al.* Guide to the Expression of Uncertainty in Measurement. 2nd Edition, International Organization for Standardization, Geneva, Switzerland, 1995.
- [4] E. O. Brigham. *The Fast Fourier Transform*, Prentice-Hall, New York, 1974.
- [5] M. G. Cox and P. M. Harris. Best Practice Guide No. 6. Uncertainty evaluation. Report, National Physical Laboratory, Teddington, UK, 2004.
- [6] P. Ciarlini, G. Regoliosi and F. Pavese. Non-parametric bootstrap with application to metrological data. In P. Ciarlini, M. G. Cox, R. Monaco, and F. Pavese, editors, *Advanced Mathematical Tools in Metrology*, 95–104, World Scientific, Singapore, 1994.
- [7] M. G. Cox, P. M. Harris and Annarita Lazzari. The applicability of non-parametric methods of statistical analysis to metrology. Report 46/04, National Physical Laboratory, Teddington, UK, 2004.

APPENDIX

The counterpart of expression (1) in terms of $C_n(\theta)$ and $S_n(\theta)$, for the ℓ th measured trace $y^{(\ell)}(\theta)$, $\ell = 1, \dots, q$, is the model equations

$$Y_n^{(\ell)}(\theta) \approx C_n(\theta - \phi_\ell) + S_n(\theta). \quad (10)$$

The use of the Fourier representations (2), (3) and (4), in conjunction with the equations (10), gives

¹² The shortest coverage interval is appropriate for all PDFs including asymmetric PDFs.

$$\begin{aligned}
& a_0^{(\ell)} + \sum_{k=1}^n \left(a_k^{(\ell)} \cos k\theta + b_k^{(\ell)} \sin k\theta \right) \\
& \approx \alpha_0 + \sum_{k=1}^n \left(\alpha_k \cos k(\theta - \phi_\ell) \right. \\
& \quad \left. + \beta_k \sin k(\theta - \phi_\ell) \right) \\
& + \gamma_0 + \sum_{k=1}^n \left(\gamma_k \cos k\theta + \delta_k \sin k\theta \right).
\end{aligned}$$

For this equation to hold for all θ , for each k the coefficients of $\cos k\theta$ on the left and right-hand sides must equate, and similarly for $\sin k\theta$. Thus,

$$\begin{aligned}
a_k^{(\ell)} & \approx \alpha_k \cos k\phi_\ell - \beta_k \sin k\phi_\ell + \gamma_k, \\
b_k^{(\ell)} & \approx \alpha_k \sin k\phi_\ell + \beta_k \cos k\phi_\ell + \delta_k, \\
& \ell = 1, \dots, q, \quad k = 1, \dots, n.
\end{aligned}$$

These overdetermined equations, for which a unique solution for the α_k , β_k , γ_k and δ_k can be found by least squares, are *separable*: they can be written as n sets of $2q$ equations. The k th set contains only the coefficients for the k th harmonic of the CFD and the ISD, and can be expressed as

$$B_k \mathbf{v}_k \approx \mathbf{u}_k = (a_k^{(1)}, b_k^{(1)}, \dots, a_k^{(q)}, b_k^{(q)})^T, \quad (11)$$

where \mathbf{u}_k is a known vector,

$$\mathbf{v}_k = (\alpha_k, \beta_k, \gamma_k, \delta_k)^T$$

is the vector of coefficients to be determined, and

$$B_k = \begin{bmatrix} R_k^{(1)} & \dots & R_k^{(q)} \\ I_2 & \dots & I_2 \end{bmatrix}^T \quad (12)$$

with

$$R_k^{(\ell)} = \begin{bmatrix} \cos k\phi_\ell & \sin k\phi_\ell \\ -\sin k\phi_\ell & \cos k\phi_\ell \end{bmatrix},$$

a known matrix. In expression (12), I_h is the identity matrix of order h . Expression (11) constitutes $2q$ equations in α_k , β_k , γ_k and δ_k and is solved by least squares for the best estimate of their values. Its explicit solution, following some algebra, is

$$\begin{aligned}
\alpha_k & = \frac{2}{q^2 - \mu_k^2} \sum_{\ell=1}^q \sum_{h=1}^q \sin \frac{k}{2} (\phi_h - \phi_\ell) A_{k,h}^{(\ell)}, \\
\beta_k & = \frac{2}{q^2 - \mu_k^2} \sum_{\ell=1}^q \sum_{h=1}^q \sin \frac{k}{2} (\phi_h - \phi_\ell) B_{k,h}^{(\ell)}, \\
\gamma_k & = \frac{2}{q^2 - \mu_k^2} \sum_{\ell=1}^q \sum_{h=1}^q \sin \frac{k}{2} (\phi_h - \phi_\ell) C_{k,h}^{(\ell)}, \\
\delta_k & = \frac{2}{q^2 - \mu_k^2} \sum_{\ell=1}^q \sum_{h=1}^q \sin \frac{k}{2} (\phi_h - \phi_\ell) D_{k,h}^{(\ell)},
\end{aligned}$$

where

$$\begin{aligned}
A_{k,h}^{(\ell)} & = a_k^{(\ell)} \sin \frac{k}{2} (\phi_h + \phi_\ell) - b_k^{(\ell)} \cos \frac{k}{2} (\phi_h + \phi_\ell), \\
B_{k,h}^{(\ell)} & = a_k^{(\ell)} \cos \frac{k}{2} (\phi_h + \phi_\ell) + b_k^{(\ell)} \sin \frac{k}{2} (\phi_h + \phi_\ell), \\
C_{k,h}^{(\ell)} & = a_k^{(\ell)} \sin \frac{k}{2} (\phi_h - \phi_\ell) - b_k^{(\ell)} \cos \frac{k}{2} (\phi_h - \phi_\ell), \\
D_{k,h}^{(\ell)} & = a_k^{(\ell)} \cos \frac{k}{2} (\phi_h - \phi_\ell) + b_k^{(\ell)} \sin \frac{k}{2} (\phi_h - \phi_\ell).
\end{aligned}$$

Moreover, the covariance matrix associated with the k th harmonic is

$$V(\mathbf{v}_k) = (2/m)u^2(y)(B_k^T B_k)^{-1},$$

which, after some matrix algebra, becomes

$$V(\mathbf{v}_k) = \frac{2}{m} \times \frac{u^2(y)}{q^2 - \mu_k^2} \begin{bmatrix} qI_2 & -\mu_k R_0^T \\ -\mu_k R_0 & qI_2 \end{bmatrix},$$

where

$$R_0 = \frac{1}{\mu_k} \begin{bmatrix} c_k & -s_k \\ s_k & c_k \end{bmatrix}.$$

Formula (5) follows in particular, and also $\text{cov}(\alpha_k, \beta_k) = \text{cov}(\gamma_k, \delta_k) = 0$. Thus using representation (3) and omitting the constant term,

$$u^2(C_n(\theta)) = \sum_{k=1}^n \left(u^2(\alpha_k) \cos^2 k\theta \right. \\ \left. + u^2(\beta_k) \sin^2 k\theta \right),$$

from which formula (6) follows. Since this result is independent of θ , it follows that for a given number n of harmonics, $u(C_n(\theta))$ is a constant, $u(C_n)$, say.

Let ρ denote the correlation coefficient associated with $C_n(\theta_{\max})$ and $C_n(\theta_{\min})$, where θ_{\max} and θ_{\min} are the angles at which $C_n(\theta)$ takes its maximum and minimum values. The standard uncertainty $u(\delta C)$ associated with δC in expression (8) is given by

$$\begin{aligned}
u^2(\delta C) & = u^2(C_n(\theta_{\max})) + u^2(C_n(\theta_{\min})) \\
& \quad - 2\rho u(C_n(\theta_{\max}))u(C_n(\theta_{\min})) = 2(1 - \rho)u^2(C_n).
\end{aligned}$$

The result (9) follows, using $|\rho| \leq 1$.

Prof. M. G. Cox, Mathematics and Scientific Computing Group, National Physical Laboratory, Teddington, Middlesex TW11 0LW, UK, Tel. +44 20 8943 6096, Fax +44, 20 8977 7091, maurice.cox@npl.co.uk

Dr. Annarita Lazzari, Mitutoyo Institute of Metrology, Mitutoyo Italiana S.r.l., Corso Europa 7, I 20020 Milan, Italy, Tel. +39 02 93578 248, Fax. +39 02 93578 250, annarita.lazzari@mitutoyo.it